20th Australasian Fluid Mechanics Conference
Perth, Australia
5-8 December 2016

A Smoothed Particle Hydrodynamics model of sediment-water mixture dispersing in quiescent water

D. Ho-Minh[1], **Jian Tong** [1] **and Danielle S. Tan** [1]

[1] Department of Mechanical Engineering,
National University of Singapore, Singapore 117575

Abstract
Sediment tailings are released underwater as part of the nodule harvesting process, and this presents a concern to environmentalists due to clouding of the water during the settling process. Thus understanding the dispersion and settling process is important to coming up with solutions to minimise environmental and ecological damage. In this paper, we present a numerical model simulating a simplified version of the dispersion process - specifically, the release of a fixed volume of pre-mixed sediment-water mixture into a larger body of quiescent water. The smoothed particle hydrodynamics (SPH) method is employed to conduct these numerical simulations, using uniformly-sized spherical particles to model the sediment-water mixture and the pure water as two different fluids. We validate the results with a table-top physical experiment; comparison with the experimental data shows good agreement in terms of the settling velocity and time, as well as qualitative characteristics observed during the dispersion process. We then investigate the effect of volumetric concentration in the sediment-water mixture in two cases of volumetric ratio of sediment to water (dilute ($< 10\%$) and highly-concentrated ($> 40\%$)), and changing the concentration-dependent properties of the sediment-water mixture accordingly. Although the numerical model is simplified and does not model the movement of individual sand particles, our results show that the initial volumetric concentration of the released sediment-water does indeed have an effect on the dispersion and settling process.

Keywords: Weakly compressible SPH, sediment-water mixture, non-Newtonian fluids.

Introduction

In recent years, mining companies have revived interest in mineral-rich nodules from the seafloor owing to great potential for collecting metals such as manganese, nickel and rare-earth elements. Nodules are scattered and unattached with sediments in the seabed. A typical mining system consisting of a platform/ship at the surface, a remotely-controlled harvester at the bottom, a riser and a tailing pipe is used for the harvesting process [8]. Harvester moves horizontally to rake/vacuum nodules, grind down, and mix them with sea water to create a slurry. The slurry is transported vertically to platform/ship via the riser and processed on land. The remaining material (tailings) is returned to the seabed by discharging at a pre-determined depth in the sea. Sediment tailings create sedimentary plumes made up suspended particles (bentonic clay, silt, sand and gravels). These plumes may spread over considerable area and will take a significant amount of time to re-settle on the seabed, causing disruption to the local ecosystem and thus resulting in an increase in environmental awareness and regulation [13]. Understanding the dispersion and settling process can consequently help the assessment of the environmental and ecological impacts caused by these activities, and is also important for engineering design [16].

Sediment flow is particulate and multi-phase in nature, hence the complication of the underlying physics of flows. Both numerical and experimental studies have been conducted on this subject. Jiang et al. [9] performed experiments to examine the characteristics of a sediment-laden jet with the sediment concentration at 0.19%. Hall et al. [7] extended this with the concentration in a range of $5.5 - 12.4\%$. Higher values up to 60% cases were investigated in [1, 7]. Besides particle concentration, studies were also carried out for other parameters such as particle size, initial jet velocity and nozzle diameter. However there were errors in the measurements and estimates made for the concentration of a sand jet. Two main reasons are that Particle Image Velocimetry (PIV) is insufficient for the measurements and bubbles have an effect on the sand concentration. It is noted that in most cases the sand-water mixture is released from a point above water surface, accelerates through the air, and achieves a specified velocity before entering water. Submerged jet experiments are presented in [2, 12, 14] to study dredged sediment release in larger scale. There is still a need of small-scale experiment with submerged releasing and detailed data showing the effect of particle-particle interaction (i.e. solid concentration).

Numerical methods (i.e. Eulerian and/or Lagrangian approach) have been used to model the dispersion and settling process of sediment. Bruel et al. [2] used Finite Element Method (FEM) to solve Reynolds-averaged Navier Stokes (RANS) equations together with a transport equation for sediment. Nguyen et al. [12] applied the mathematical treatment to obtain two sets of governing equations for water and sand phases. One term which describes the interphase momentum transfer was added in the momentum equation of each phase. Calculation of this term at interfaces using FEM is complicated and requires a large amounts of computation and data storage. Saremi and Jensen [14] suggested a CFD drift-flux model which assumes sand-water mixture as a whole, resulting one only has to solve one set of equation for mixture rather than two sets for two phases separately. Continuous models like CFD are extensively used in many two-phase problems because their results are generally non-disputed. However, continuous models (e.g. drift-flux) require some constitution assumptions which omit some characteristics of two-phase flow such as particle-particle interactions and microscopic structures. Particle-based (Lagrangian approach) methods have been adopted to this subject and expected to give better results than mesh-based methods. Shakibaeinia and Jin [15] applied the Moving Particle Semi-implicit (MPS) method to model sand discharge in still water. Combined with rheological model, MPS is capable to capture some flow features of sand. Smoothed Particle Hydrodynamics (SPH) is widely used owing to its well-developed foundation over time. Reports in studies of sediment-water solid-fluid flows [5, 11] indicate that SPH is ideal for interfacial and highly non-linear flows with fragmentation and re-suspension. However, there is no report on SPH modelling of submerged jet and dispersion process of sediment, especially in deep-sea conditions.

In this study, a non-Newtonian two-phase model, based on the weakly compressible SPH (WC-SPH) formulations, is employed to model sediment falling underwater. Referring to [15],

we use spherical particles of equal size to model the sediment-water mixture and the pure water as two different fluids according to the volumetric concentration of sediment in mixture. In other words, each particle carries a certain sediment concentration which is initially assigned and fixed during the simulation. Figure 1 is an illustration of sediment-water mixture represented by particles. To consider non-Newtonian behaviour of mixture, the effective viscosity of the mixture is determined as a function dependent on the local sediment concentration. Numerical results are then validated with data obtained from experiments.

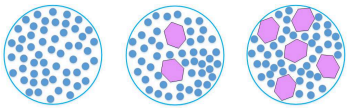

a) b) c)

Figure 1: Definition of sediment-water mixture represented by particles: a) pure water particle; b) sediment-water particle for a dilute case; c) sediment-water particle for a concentrated case

SPH implementation

The continuity equations and the momentum equations in a Lagrangian frame take the forms

$$\frac{d\rho}{dt}+\rho\frac{\partial u^{\alpha}}{\partial x^{\alpha}}=0, \tag{1}$$

$$\frac{du^{\alpha}}{dt}=\frac{1}{\rho}\frac{\partial \sigma^{\alpha\beta}}{\partial x^{\beta}}+g^{\alpha}, \tag{2}$$

where α and β denote coordination direction, ρ the density, u the velocity vector, g the gravitational force and σ the total stress tensor. The total stress tensor can be decomposed into

$$\sigma^{\alpha\beta}=-p\delta^{\alpha\beta}+f(D^{\alpha\beta}), \tag{3}$$

where p is the isotropic pressure, $\delta^{\alpha\beta}$ the Kronecker delta and $D^{\alpha\beta}$ the strain rate tensor which is defined as

$$D^{\alpha\beta}=\frac{1}{2}\left[\frac{\partial u^{\alpha}}{\partial x^{\beta}}+\frac{\partial u^{\beta}}{\partial x^{\alpha}}\right]. \tag{4}$$

In case of Newtonian fluid,

$$f(D^{\alpha\beta})=2\mu D^{\alpha\beta}, \tag{5}$$

where μ is the dynamic viscosity. The discretised forms of (1) and (2) are

$$\frac{d\rho_i}{dt}=\rho_i\sum_{j}^{N}\frac{m_j}{\rho_j}\left(u_i^{\alpha}-u_j^{\alpha}\right)\frac{\partial W_{ij}}{\partial x^{\alpha}}, \tag{6}$$

$$\frac{du_i^{\alpha}}{dt}=\sum_{j}^{N}m_j\left(\frac{\sigma_i^{\alpha\beta}+\sigma_j^{\alpha\beta}}{\rho_i\rho_j}\right)\frac{\partial W_{ij}}{\partial x^{\beta}}+g_i^{\alpha}. \tag{7}$$

The quintic Wendland kernel [17] used in this discretisation is in this form

$$W_{ij}=\frac{7}{4\pi h^2}\left(1-\frac{q}{2}\right)^4(2q+1), \qquad 0\le q\le 2, \tag{8}$$

where $q=r_{ij}/h$, r_{ij} is the absolute distance between particle i and j, and h the smoothing length.

In WCSPH approach, the pressure is calculated from equation of state which is called Taits' equation

$$p=B\left(\left(\frac{\rho}{\rho_0}\right)^{\gamma}-1\right), \tag{9}$$

where ρ_0 is the reference density, γ the polytrophic index ($\gamma=7$ for fluid [3] in this study) and B a constant which is determined from the speed of sound, c_{s0}, as $B=c_{s0}^2\rho_0/\gamma$. $c_{s0}=10u_{\max}$ with $u_{\max}$ the maximum velocity in the domain. Once the speed of sound of pure water is determined, the speed of sound of mixture is obtained by the following ratio [3]

$$\frac{c_{s,X}}{c_{s,Y}}=\sqrt{\frac{\rho_{0,Y}\gamma_X}{\rho_{0,X}\gamma_Y}}, \tag{10}$$

where X,Y stand for pure water and mixture, respectively. Equation (7) is rewritten

$$\begin{aligned}\frac{du_i^{\alpha}}{dt} &= \sum_{j}^{N}m_j\left(\frac{p_i}{\rho_i^2}+\frac{p_j}{\rho_j^2}\right)\frac{\partial W_{ij}}{\partial x^{\beta}}\\ &+ \sum_{j}^{N}\frac{m_j}{\rho_i\rho_j}\frac{4\mu_i\mu_j}{\mu_i+\mu_j}u_{ij}^{\alpha}\frac{x_{ij}^{\alpha}\cdot\frac{\partial W_{ij}}{\partial x^{\beta}}}{\left(x_{ij}^{\alpha}\right)^2+0.01h^2}+g_i^{\alpha}.\end{aligned} \tag{11}$$

If particle i or j is pure water, the dynamic viscosity $\mu=\mu_w=10^{-3}$ Pa.s and unchanged during the simulation. For mixture particles, we employ a Krieger-Dougherty equation [10] to represent mixture viscosity

$$\mu_i=\mu_w\left(1-\frac{\phi_i}{\phi_{\max}}\right)^{(-2.5\phi_{\max})}, \tag{12}$$

where ϕ_i is the local concentration, and $\phi_{\max}$ is the maximum local concentration. Instead of using the convection-diffusion equation of sediment transport to obtain concentration values, the local volumetric concentration of mixture in a volume V can be expressed in the form

$$\phi_i=\phi_0\frac{\sum_{j\in J}\frac{m_j}{\rho_j}}{\sum_{j\neq i}\frac{m_j}{\rho_j}}, \tag{13}$$

where ϕ_0 is the initially assigned concentration and J is total number of mixture particles in V.

Experimental and numerical results

Figure 2 shows a sketch of experiment setup. The experiments were performed in a glass tank 430 mm long by 195 mm wide by 250 mm high. The tank was filled with water. The discharge was executed through a conical funnel with an opening of diameter 84 mm at the top, height of 90 mm and a narrow opening of diameter of 8 mm at the bottom. The funnel has a volume of 0.166 liter and was filled with water and silica sand (effective diameters from 100 μm to 500 μm). The opening was positioned 170 mm above the tank base. A valve/plug at the bottom of funnel is used to control the releasing of sand-water mixture into still water in the tank. We used a Photron Fastcam SA5 to record the dispersion and settling process. The video is then processed by Photron Fastcam Analysis software to extract photographs and data (e.g. average falling time, position and dimension of sediment cloud). Three light sources were used: one in front of the tank and two at the side, aimed towards the back. Two cases of dilute and dense sand concentration are considered, details of experiments are shown in Table

1. Here the concentration by volume C_v is calculated from the concentration by mass C_m by $C_v = 1/\left(1+\rho_s/\rho_w\left(1/C_m-1\right)\right)$ where ρ_w and ρ_s are the density of water and sand, respectively. The densities of mixture, ρ_m, are then obtained by $\rho_m = C_v\rho_s + (1-C_v)\rho_w$. The initial sand velocity at the opening, u_0, is predicted by Torricelli's law $u_0 = \sqrt{2gH}$ where g is the acceleration due to gravity, and H the height of funnel. Therefore the Reynolds number $\mathrm{Re} = \rho_w u_0 d/\mu_w$ and the Froude number $\mathrm{Fr} = u_0/\left(gd\left(\rho_s-\rho_w\right)/\rho_w\right)^{1/2}$ with d being the diameter of the opening of funnel.

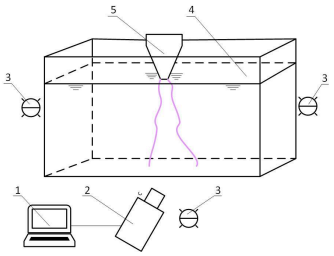

Figure 2: Arrangement for experiments: 1. Computer; 2. High-speed camera; 3. Light sources; 4. Water tank; 5. Funnel with valve

Figure 3 shows the computational domain in 2D and initial particle configuration. To reduce the cost of computing, only an area (300 mm by 300 mm) at the center of the tank is considered. Therefore, periodic boundary conditions are applied at left and right boundaries. Dynamic boundary conditions [4] have been implemented at the solid boundaries at the base of the tank and the walls of funnel. The number of SPH particles (cyan) representing pure water is 28358. The sand-water mixture is modelled by 2071 SPH particles (magenta). The system of equation (6), (11) and (12) is solved by the open-source SPHYSICS [6] with a modification which makes it capable of solving multi-phase problems.

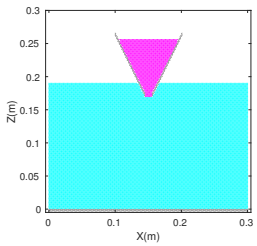

Figure 3: Computational domain and initial particle configuration

Properties of sand and water		
Sand's median diameter D_{50}, (μm)	Density of sand ρ_s, (kg/m^3)	Density of water ρ_w, (kg/m^3)
300	2540	1000

Properties of mixture		
Concentration by mass C_m, (%)	Concentration by volume C_v, (%)	Density of mixture ρ_m, (kg/m^3)
20	8.96	1138
80	61.16	1942

Initial flow characteristics		
Initial sand velocity u_0, (m/s)	Reynolds number Re	Froude number Fr
1.33	10640	3.83

Table 1: Experimental conditions

There are three stages of dispersion of sand-water mixture in water: i) Falling: The mixture forms a cloud that moves downward due to gravity; ii) Impacting: The cloud hits the base; and iii) Spreading: The cloud receives energy from impacts and spreads horizontally. In this work, only the falling stage is reported. After opening the valve/plug, the mixture descends into the tank and accelerates. This flow then forms vortices on both sides of the centre line, resulting in particles close to a vortex moving sideways and slightly upwards in a cyclical pattern. The mixture particles near centre line reach the maximum velocity and move mostly downward. The leading particles in mixture flow create a formation similar to a cloud/swarm which is falling and growing as time increases. In this paper, position of leading edge and horizontal cloud diameter are two parameters for quantitative comparison between 2D simulations and 3D experiments. Figure 4 shows the evolution of this cloud in terms of position of the front, and width of the cloud. Dashed lines represent empirical results, while smooth lines represent numerical results. We see that there is good agreement in terms of the leading edge of the cloud, which shows that the SPH simulation can predict the falling time for both cases of low and dense sand concentration (see Figure 4a). The growth of cloud is shown in Figure 4b. In the case of low sand concentration, the numerical results match experimental results at the middle and the end of falling stage. However, SPH model over-estimates the maximum diameter of cloud at the beginning. In the case of dense sand concentration, the gap between predicted and measured data is still high. These differences are likely to be due to the radial velocities of mixture particles in SPH simulation being higher than that of experiments possibly due to greater level of compaction in the simulations. Thus the growth rate of the cloud increases and the cloud has bigger size.

Figure 5 shows time history of dilute and concentrated flows of sand-water mixture for both the numerical and physical experiments. Snapshots of both are taken at similar times for consistency in comparison. We observe that the numerical simulation exhibits fairly good agreement with the physical experiments, especially for the dilute case. Generally, the frontal edge of cloud has a bowl shape. Its formation is the result of the interaction between the vortical flow and the suspended sand particles. The size and shape of the cloud depends on the volumetric concentration of sand. When the concentration is low, the tail of the cloud looks like a cone with the narrowest part at the opening of funnel (see Figure 5a). In the case of high concentration, the particle grouping effect (i.e. higher density) enhances the axial velocity, the particles move mostly along the axial direction and disperse very little along the radial direction. The vortices are thus reduced in the magnitude, resulting in the frontal and tail of the cloud being smaller than those of low concentration case (see Figure 5b). However for both numerical and physical experiments, owing to higher values of relative velocity, denser cloud takes shorter time to reach the base. Our 2D SPH simulation predicted the qualities of the sedimentation fairly well, but there are some reasonable differences (i.e. the larger diameter of the cloud, the wider tail of the cloud) in comparison with 3D experiments.

Conclusion

The performance of a simple SPH approach for simulating the falling stage of sand-water mixture has been compared against with experimental results in this paper. The mixture is treated as a heavier fluid whose viscosity is calculated from suspension viscosity model. Two cases of dilute and highly-concentrated flows are examined. For the former, promising results are obtained when SPH model is capable of predicting the falling and dispersion of sand. For the latter, some improvements are needed to capture more accurately the growth of sand cloud (i.e. internal vortical flows due to particle-particle interaction). This approach combined with non-Newtonian rheology for dense flows is currently under investigation and will be reported in future work.

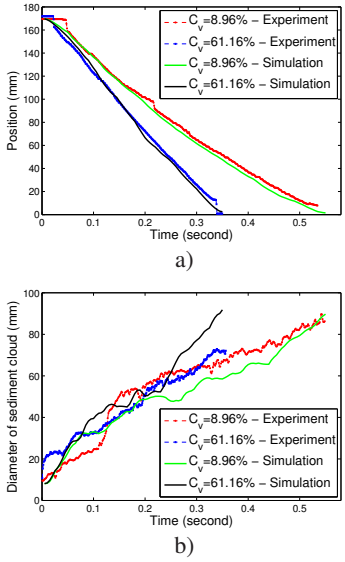

Figure 4: Mixture cloud evolution: a) Position of the leading edge of the cloud; b) Maximum diameter of the cloud

Acknowledgements

This work was funded by the Singapore Ministry of Education (MOE) AcRF Grant, WBS no. R-265-000-508-133.

References

[1] Azimi, A. H., *Experimental and Numerical Investigations of Sand-Water Slurry Jets in Water*, Ph.D. thesis, University of Alberta, 2012.

[2] Burel, D. and Garapon, A., 3D numerical modelling of dredged material descent, in *Proceedings of the 28th International Conference - Coastal Engineering 2002*, editor J. M. Smith, 2002.

[3] Colagrossi, A. and Landrini, M., Numerical simulation of interfacial flows by Smoothed Particle Hydrodynamics, *Journal of Computational Physics*.

[4] Crespo, A., Gomez-Gesteira, M. and Dalrymple, R., Boundary conditions generated by dynamic particles in SPH methods, *Computers, materials & continua*, **5**, 2007, 173–184.

[5] Fourtakas, G. and Rogers, B. D., Modelling multi-phase liquid-sediment scour and resuspension induced by rapid flows using Smoothed Particle Hydrodynamics (SPH) accelerated with a Graphics Processing Unit (GPU), *Advances in Water Resources*, **92**, 2016, 186–199.

[6] Gomez-Gesteira, M., Crespo, A., Rogers, B., Dalrymple, R., Dominguez, J. and Barreiro, A., SPHYSICS - development of a free-surface fluid solver- part 2: Efficiency and test cases, *Computers & Geosciences*, **48**, 2012, 300–307.

[7] Hall, N., Elenany, M., Zhu, D. Z. and Rajaratnam, N., Experimental study of sand and slurry jets in water, *Journal of Hydraulic Engineering*, **136**, 2010, 727–738.

[8] Jankowski, J. and Zielke, W., The mesoscale sediment transport due to technical activities in the deep sea, *Deep-Sea Research II*, **48**, 2001, 3487–3521.

[9] Jiang, J., Law, A. W.-K. and Cheng, N.-S., Two-phase analysis of vertical sediment-laden jets, *Journal of Engineering Mechanics*, **131**, 2005, 308–318.

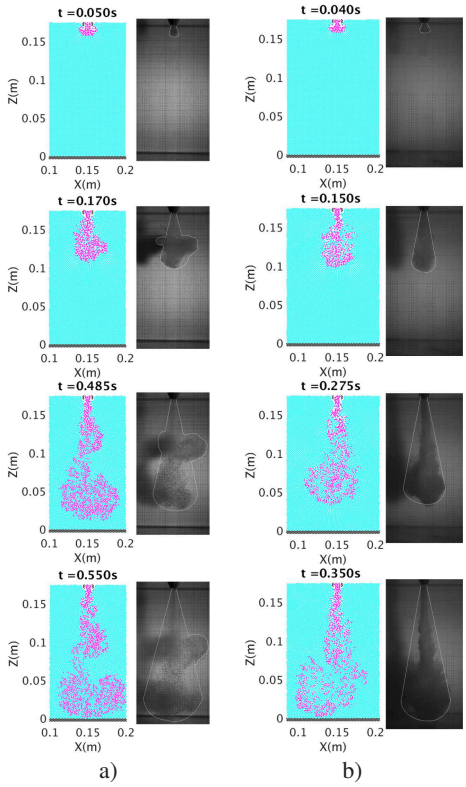

Figure 5: Numerical and experimental results of sediment-water flow at a) low concentration b) dense concentration. Dashed lines have been added on the experiment photos to clarify the general shape of the sediment-water flow.

[10] Krieger, I. and Dougherty, T., A mechanism for non-Newtonian flow in suspensions of rigid spheres, *Transactions of Society of Rheology*, **3**.

[11] Manenti, S., Sibilla, S., Gallati, M., Agate, G. and Guandalini, R., SPH simulation of sediment flushing induced by a rapid water flow, *Journal of Hydraulic Engineering*, **138**, 2012, 272–284.

[12] Nguyen, D., Levy, F., Pham Van Bang, D., Guillou, S. and Nguyen, K., Simulation of dredged sediment releases into homogeneous water using a two-phase model, *Advances in Water Resources*, **48**, 2012, 102–112.

[13] Rolinski, S., Segschneider, J. and Sundermann, J., Long-term propagation oftailings from deep-sea mining under variable conditions by means of numerical simulations, *Deep-Sea Research II*, **48**, 2001, 3465–3485.

[14] Saremi, S. and Hjelmager Jensen, J., Multiphase CFD modeling of nearfield fate of sediment plumes, in *3rd IAHR Europe Congress, Book of Proceedings*, 2014.

[15] Shakibaeinia, A. and Jin, Y.-C., Lagrangian multiphase modeling of sand discharge into still water, *Advances in Water Resources*, **48**, 2012, 55–67.

[16] Thiel, H. and Tiefdee-Umweltschutz, F., Evaluation of evironmental consequences of polymetalic nodule mining based on the results of the TUSCH reseach association, *Deep Sea Research II*, **48**, 2001, 3433.

[17] Wendland, H., Piecewise polynomial, positive definite and compactly supported radial functions of minimal degree, *Advances in Computational Mathematics*, **4**, 1995, 389–396.